Bioorganic & Medicinal Chemistry 18 (2010) 6725–6733

Contents lists available at ScienceDirect

Bioorganic & Medicinal Chemistry

journal homepage: www.elsevier.com/locate/bmc

Bisbibenzyl derivatives sensitize vincristine-resistant KB/VCR cells to chemotherapeutic agents by retarding *P*-gp activity

Guang-min Xi [a,†], Bin Sun [b,†], Hui-hui Jiang [a], Feng Kong [a], Hui-qing Yuan [a,*], Hong-xiang Lou [b,*]

[a] Department of Biochemistry and Molecular Biology, School of Medicine, Shandong University, Jinan, Shandong 250012, PR China
[b] Department of Natural Product Chemistry, School of Pharmaceutical Sciences, Shandong University, Jinan 250012, PR China

ARTICLE INFO

Article history:
Received 8 June 2010
Revised 22 July 2010
Accepted 23 July 2010
Available online 29 July 2010

Keywords:
Marchantin C
Derivatives
Multidrug resistance
P-glycoprotein
Apoptosis
KB/VCR cells

ABSTRACT

P-glycoprotein (*P*-gp) is known to mediate multidrug resistance (MDR) by acting as an efflux pump to actively transport chemotherapeutic agents out of carcinoma cells. Inhibition of *P*-gp function may represent one of the strategies to reverse MDR. We have previously reported that marchantin C (MC), a macrocyclic bisbibenzyl compound from liverworts, exerts anti-tumor activity as an antimitotic agent. This study was designed to evaluate the possible modulatory effect of MC and its three synthetic derivatives (MC1, MC2 and MC3) on *P*-gp in VCR-resistant KB/VCR cells. Results of the cytotoxicity assay revealed that MC was the most potent inhibitor of cell proliferation in both KB and KB/VCR cells among these four compounds, while the three MC-derived chemicals had little anti-proliferative activity under the same condition. However, in *P*-gp-expressing MDR cells, analysis of potency of these compounds in enhancing cytotoxicity of VCR led to the identification of MC2 as a more effective chemical on reversal of resistance. Further study showed that MC2 was able to reduce efflux of rhodamine-123, and in turn, increase the accumulation of rhodamine-123 and adriamycin in KB/VCR cells, indicating that MC2 re-sensitized cells to VCR by inhibition of the *P*-gp transport activity. In addition, the combination of MC2 and VCR at a concentration that does not inhibit cell growth resulted in an induction of apoptosis in KB/VCR cells. These results suggest that MC2, as a novel and effective inhibitor of *P*-gp, may find potential application as an adjunctive agent with conventional chemotherapeutic drugs to reverse MDR in *P*-gp overexpressing cancer cells.

1. Introduction

Chemotherapy plays a very important role in the treatment of malignant tumors. However, the occurrence of the multidrug resistance (MDR) still represents a major obstacle for successful cancer chemotherapy. Multidrug resistance is a phenomenon in which cancer cells exposed to one anticancer drug become resistant to other chemotherapeutic drugs whose structures and functions are unrelated with each other.[1–3] Although several cellular mechanisms are associated with the development of MDR, including the reduction of apoptosis, activation of DNA damage repair systems and alteration of drug metabolism, *P*-glycoprotein (*P*-gp), an ATP-binding cassette (ABC) transporter, is the most extensively characterized mediator of MDR.[4] *P*-gp is capable of extruding various drugs from cells in an energy-dependent manner, leading to decreased drug concentrations within the cell and reduced efficacy of drugs. Therefore, numerous efforts have been made to develop compounds capable of modulating the activity of *P*-gp in order to reverse the MDR phenotype.[5,6] A number of noncytotoxic drugs which sensitize MDR cells to chemotherapeutic drugs have been identified, including calcium channel blockers (verapamil, nifedipine), calmodulin antagonists (trifluoperazine chlorpromazine), and immunosuppressive drugs (cyclosporine A, rapamycin). Naturally occurring polyphenolic compounds, such as curcuminoids, curcumin and epigallocatechin 3-gallate (EGCG) have also been reported to block drug efflux and reverse MDR phenotype.[7–9] However, these compounds failed in clinical trials because of their severe side effects and poor pharmacokinetics in vivo.[1] Therefore, the development of safe and effective MDR reversal agents is an important approach to reversing clinical MDR.

Macrocyclic bisbibenzyls, a class of liverwort-derived natural chemicals, have diverse biological activities, including cytotoxic, antioxidant, antibacterial and antifungal activity.[10–12] Marchantin C (MC) (Fig. 1), a natural macrocyclic bisbibenzyl, was first isolated

Abbreviations: ADR, adriamycin; MDR, multidrug resistance; MTT, 3-(4,5-dimethylthiazol-2-yl)-2,5-diphenyl-2*H*-tetrazolium bromide; *P*-gp, *P*-glycoprotein; Rh123, rhodamine-123; VCR, vincristine; VRP, verapamil.

* Corresponding authors. Tel.: +86 531 88382092; fax: +86 531 88382019 (H.Q.Y.).
E-mail addresses: lyuanhq@sdu.edu.cn (H. Yuan), louhongxiang@sdu.edu.cn (H. Lou).

† These authors contributed equally to this work.

0968-0896/$ - see front matter © 2010 Elsevier Ltd. All rights reserved.
doi:10.1016/j.bmc.2010.07.055

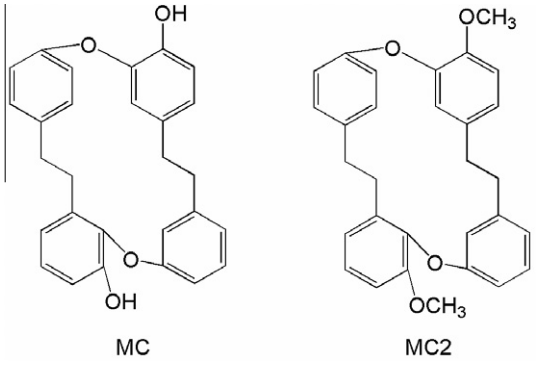

Figure 1. Chemical Structures of MC and MC2.

from liverworts *Marchantia polymorpha* by Asakawa et al. in 1983.[13] It was previous found to be an excellent cytotoxic agent against KB and P388 leukemia cell lines, and also displayed anti-HIV, antibacterial, DNA polymerase β inhibitory, iNOS inhibitory and α-glucosidase inhibitory activities.[14–18] Recently, our group found marchantin C could induce apoptosis of tumor cells as an antimitotic agent.[19,20]

The potent anti-tumor activity of MC and limited natural resources motivated us to prepare it by total synthesis and analyzed its possible structure-mediated anti-tumor activity. In the present study, we synthesized MC (**16**) as well as its three cyclic synthetic derivatives, dimethyl ether of dehydromarchantin C (MC1, compound **13**), dimethyl ether of marchantin C (MC2, compound **14**), and dehydromarchantin C (MC3, compound **15**) in a satisfactory yield, and examined their effects on both drug-sensitive and drug-resistant cancer cells. The results indicated that these compounds potentiated the cytotoxicity of VCR and inhibited *P*-gp activity in KB/VCR cells.

2. Results and discussion

2.1. Synthesis of marchantin C and its derivatives

We have focused on the efficient total synthesis of marchantin C for a long time. Although a total synthesis of marchantin C was reported in *Tetrahedron Letters* recently,[21] herein we report another efficient method to marchantin C in 12 steps with a total yield of 23%.

The total synthesis of marchantin C was achieved as shown in Scheme 1. The synthetic route began with the Ullmann coupling of the protected 2-hydroxy-3-methoxybenzaldehyde (**2**) with commercially available 3-bromo-benzaldehyde, resulting in the formation of the diphenyl ether **3**. The phosphonium salt **8**, as the second diphenyl ether building block, was synthesized in a conventional sequence starting with S_NAr displacement of methyl 4-bromobenzoate (**5**) by 3-hydroxy-4-methoxybenzaldehyde (**4**) to give the diphenyl ether **6**. Compound **6** was then reduced with sodium borohydride to give the benzyl alcohol **7**, followed by reaction with triphenylphosphonium bromide, affording **8** in three steps. The building blocks **3** and **8** were combined by Wittig reaction in the presence of potassium carbonate and 18-crown-6, and the stilbene **9** (obtained as *E*/*Z* mixture) was hydrogenated over Pd/C to give the bibenzyl **10**. Next, the carboxylic ester group of **10** was reduced with lithium aluminium hydride, followed by deprotection with HCl/H_2O to yield compound **11**. Again the reaction of **11** with triphenylphosphonium bromide afforded compound **12**. Cyclization of **12** by means of an intramolecular Wittig reaction was achieved with sodium methoxide, leading to key macrocyclic intermediate **13**. Finally, **13** could be demethylated by boron tribromide at −78 °C to give phenol **15** or hydrogenated to give dimethyl marchantin C (**14**), followed by demethylation to afford marchantin C (**16**).

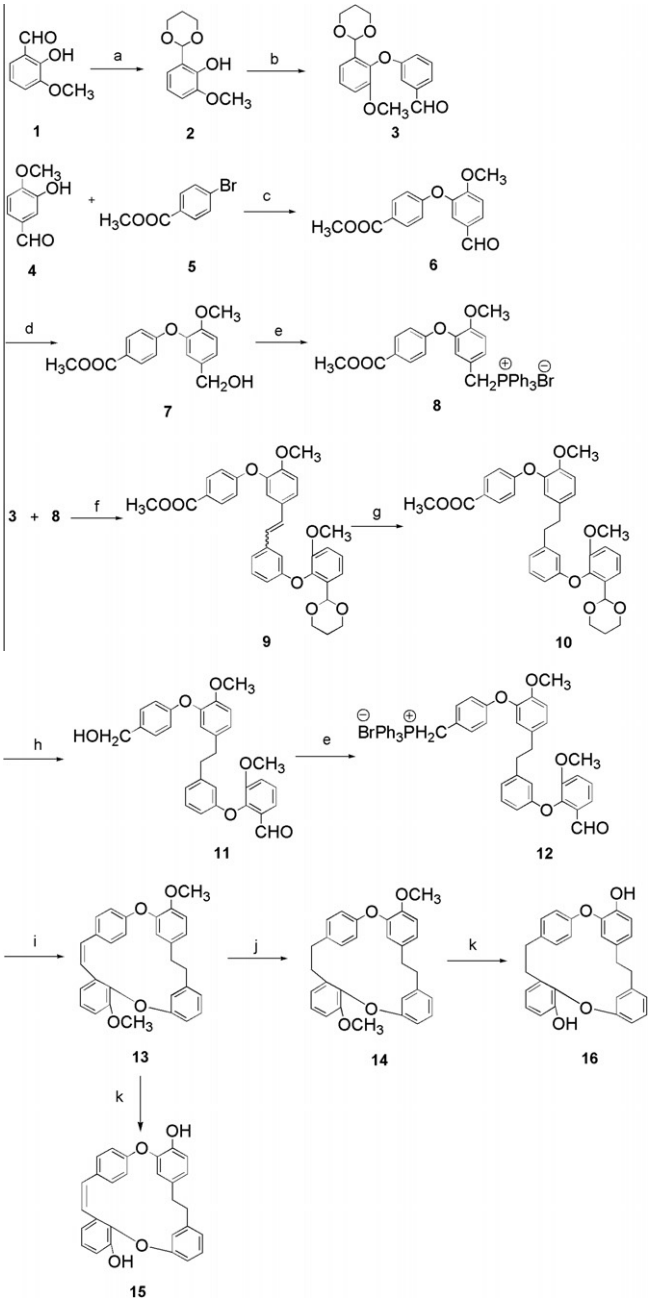

Scheme 1. Synthesis of marchantin C. Reagents and conditions: (a) 1,3-propanediol, DMS–DMF, DCM; (b) 3-bromo-benzaldehyde, K_2CO_3, CuO, Pyridine, reflux; (c) K_2CO_3, pyridine, CuO, reflux; (d) $NaBH_4$, THF, rt; (e)PPh_3·HBr, CH_3CN, reflux; (f) K_2CO_3, 18-crown-6, CH_2Cl_2, reflux; (g) H_2, 10% Pd/C, Et_3N, AcOEt, rt; (h) (1) $LiAlH_4$, THF, 30 °C; (2) H^+/H_2O, rt; (i) NaOMe, CH_2Cl_2, rt; (j) H_2, 10% Pd/C, AcOEt, rt; (k) BBr_3, CH_2Cl_2, −78 °C.

2.2. Cytotoxicity of marchantin C and its derivatives in KB and KB/VCR cells

In our previous study, we reported that MC could trigger apoptosis in various cultured tumor cells.[19,20] Therefore, we firstly investigated the cytotoxic effects of MC and its derivatives on KB and KB/VCR cells with MTT assay. As shown in Figure 2, treatment of cells with MC led to a profound cell viability inhibition in a dose-

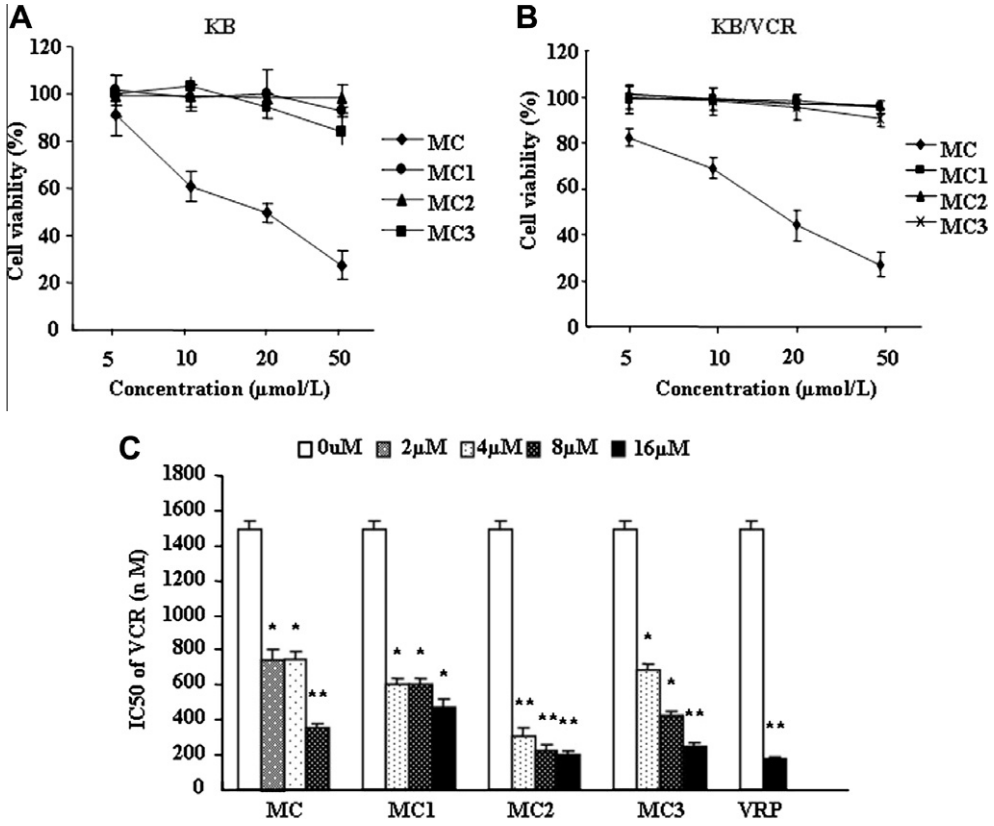

Figure 2. (A) Effects of MC and it's derivatives on the growth of KB cells. (B) Effects of MC and it's derivatives on the growth of KB/VCR cells. The cells were treated with various concentrations of these compounds for 48 h. Viable cell numbers were evaluated by MTT assay and were denoted as a percentage of DMSO treated controls at the concurrent time point. (C) Reversal effect of MC and it's derivatives on the KB/VCR cells. The cells were exposed to VCR at presence of these four compounds. IC_{50} values for VCR were calculated. Data from three independent experiments were shown as means ± SD. $^{*}P$ <0.05, $^{**}P$ <0.01 versus VCR treatment alone.

dependent manner. The IC_{50} value of MC in KB cells was 16.48 ± 1.17 μM, and in KB/VCR the value was 17.47 ± 1.14 μM. However, unlike MC, MC1, MC2 and MC3 ranged from 5 to 50 μM had no significant inhibitory effects on the growth of both KB and KB/VCR cells. The IC_{50} values of MC1, MC2 and MC3 were 93.48 ± 3.71, 94.85 ± 2.09, and 83.98 ± 3.82 μM for KB cells, and 88.51 ± 2.02, 95.38 ± 1.92, and 86.88 ± 2.06 μM for KB/VCR cells, respectively. These results suggested that both drug-resistant and parental cells were more sensitive to MC than MC derivatives. In addition, KB/VCR cells showed slightly resistant to MC.

2.3. Marchantin C and its derivatives potentiate the cytotoxicity of chemotherapeutic agents in KB/VCR cells

To investigate the effect of MC and its derivatives on the sensitivity of cells to chemotherapeutic agent, we performed MTT assay to determine the VCR cytotoxic effect with or without pretreatment of these compounds. The results showed that these four compounds were potent to reverse the VCR-associated MDR phenotype in KB/VCR cells (Table 1, Fig. 2C). VCR-mediated cytotoxicity was drastically increased, and the IC_{50} values of VCR toward KB/VCR were decreased in the presence of these compounds. The fold reversal of resistance to VCR upon exposure to MC (8 μM), MC1, MC2, MC3 (16 μM) was 4.2, 3.1, 7.5, 6.0, respectively. The data indicated that MC and its derivatives had the ability to sensitize drug-resistant cells to VCR. Moreover, this led to the selection of MC2 as a potent modulator for further mechanistic studies. Table 2 showed the IC_{50} of VCR and the fold reversal of resistance in the presence of MC2. The data revealed that the IC_{50} of VCR decreased drastically from 1483.48 to 196.95 nM in the presence of MC2 at 16 μM, producing a 7.5-fold reduction in the IC_{50} of VCR in KB/VCR cells. The effect was dose-dependent—an increasing concentration of MC2 correlated with a decreased IC_{50} of VCR. However, this effect of MC2 was less evident in drug-sensitive KB cells lacking *P*-gp (Table 2).

Table 1
Effects of MC and its synthetic derivatives on the cytotoxicity of VCR in KB/VCR cells

Treatment	IC_{50} (nmol/L)	RF[b]
VCR	1483.48 ± 50.18	–
VCR + MC (2 μM)	743.54 ± 65.18	1.99
VCR + MC (4 μM)	625.03 ± 51.69	2.37
VCR + MC (8 μM)	354.01 ± 28.97	4.19
VCR + MC1 (4 μM)	600.79 ± 41.13	2.47
VCR + MC2 (8 μM)	575.62 ± 34.66	2.57
VCR + MC1 (16 μM)	478.78 ± 40.54	3.10
VCR + MC2 (4 μM)	310.06 ± 47.51	4.78
VCR + MC2 (8 μM)	219.40 ± 42.49	6.76
VCR + MC2 (16 μM)	196.95 ± 25.06	7.53
VCR + MC3 (4 μM)	688.71 ± 37.87	2.16
VCR + MC3 (8 μM)	423.89 ± 28.41	3.51
VCR + MC3 (16 μM)	250.32 ± 25.70	5.95
VCR + VRP (16 μM)	167.52 ± 14.83	8.85

[a] Cell survival was determined by MTT assay. Values are means ± SD of three experiments.
[b] The reversal activity of target compounds was expressed reversal folds (RF). RF = IC_{50} of VCR alone/IC_{50} of VCR in the presence of test compounds.

ADR, another substrate of *P*-gp with different modes of action that is structurally unrelated to VCR, was employed to confirm the reversal activity of MC2 in KB/VCR cells. As shown in Table 2, the IC_{50} value of ADR was reduced 6.1-fold in KB/VCR cells exposed

Table 2
Potency of MC2 in promoting cytotoxicity of VCR and ADR in KB and KB/VCR cells[a]

Treatment	KB		KB/VCR	
	IC_{50}	RF	IC_{50}	RF
VCR (nM)	6.07 ± 0.68	—	1489.58 ± 50.18	—
VCR + MC2 (4 μM)	5.20 ± 0.45	1.17	310.05 ± 47.51	4.78
VCR + MC2 (8 μM)	4.56 ± 0.32	1.33	219. 40 ± 42.49	6.76
VCR + MC2 (16 μM)	3.93 ± 0.19	1.54	196.95 ± 25.06	7.53
VCR + VRP (16 μM)	4.70 ± 0.18	1.29	176.84 ± 14.83	8.85
ADR (μg/ml)	1.66 ± 0.53	—	49.66 ± 2.61	—
ADR + MC2 (4 μM)	1.62 ± 0.44	1.02	12.53 ± 1.46	3.96
ADR + MC2 (8 μM)	1.44 ± 0.25	1.15	11.82 ± 1.31	4.20
ADR + MC2 (16 μM)	1.83 ± 0.16	0.91	8.19 ± 0.87	6.06
ADR + VRP (16 μM)	1.56 ± 0.40	1.06	9.34 ± 0.77	5.32

[a] KB/VCR cells were exposed to anticancer drugs in the presence of MC2 or VRP for 48 h and IC_{50} (concentration inhibiting 50% growth) was determined by MTT assay. Values are means ± SD of three experiments.

to MC2 at a concentration of 16 μM. However, neither of the VRP nor MC2 significantly affected the IC_{50} of ADR in the parental KB cells. These observations suggested that these compounds were able to reverse MDR via *P*-gp inhibition.

2.4. The effect of MC2 on *P*-gp expression

The reversal of *P*-gp-mediated MDR can be achieved either by decreasing *P*-gp expression or by inhibiting its drug-transport activity. We incubated KB/VCR cells with MC2 at 4, 8, and 16 μM for 48 h, and examined the change in *P*-gp protein abundance. The results of the Western blot shown in Figure 3A, revealed that the protein level of *P*-gp was not altered by MC2 treatment in KB/VCR cells. These results indicated that reversal of resistance by MC2 may be attributed to the inhibition of *P*-gp function.

2.5. MC2 causes accumulation of ADR and Rh123 in KB/VCR cells

The fluorescence characteristics of ADR were utilized to determine intracellular drug concentration by flow cytometry. The ability of MC2 to inhibit P-gp-mediated transport was examined by determining the intracellular ADR-associated fluorescence intensity in KB/VCR cells. As shown in Figure 3B, the accumulation of ADR in KB cells was evident in either untreated or treated cells. Whereas, the accumulation of ADR in KB/VCR cells was significantly lower than that in KB cells. After the treatment with 4, 8, 16 μM of MC2 for 1 h, respectively, intracellular accumulation of ADR was increased 2.1-, 2.8-, and 5.7-fold in comparison with DMSO-treated control cells (p <0.05). These results suggested that MC2 elevated the sensitivity of KB/VCR cells toward chemotherapeutics through increasing chemotherapeutics accumulation inside KB/VCR cells.

To further confirm the ability of MC2 to inhibit *P*-gp-mediated transport, we investigated the effect of MC2 on transport of Rh123, another well-established fluorescent substrate of *P*-gp. Consistent with the results shown in Figure 3B, Rh123 in KB cells was not affected by MC2 or VRP treatment (Fig. 3C), however, MC2 treatment induced a marked accumulation of Rh123 in KB/VCR cells in a dose-dependent manner. These observations suggested that the reversal of resistance to VCR and ADR is *P*-gp specific.

2.6. MC2 inhibits *P*-gp-mediated efflux

Subsequently, we performed experiments to determine whether the increased accumulation of Rh123 in the KB/VCR cells was due to inhibition of Rh123 efflux. The time course of Rh123 efflux in the presence MC2 (16 μM) was analyzed by flow cytometry. The results in Figure 3D demonstrated that without MC2, a rapid decrease of intracellular Rh123 was observed in KB/VCR cells after incubation in Rh123-free medium for 120 min. However, in the presence of MC2, Rh123 efflux was drastically suppressed in KB/VCR cells. In addition, like VRP, duration of action of MC2 was short and reversible because the intracellular Rh123 was not retained for 120 min (Fig. 3D). These results suggest that MC2 increased chemotherapeutics accumulation inside KB/VCR cells through inhibiting outward transport function of *P*-gp.

2.7. Treatment with MC2 and VCR induces apoptosis in KB/VCR cells

To determine whether the observed cell death caused by the co-treatment of the cells with VCR and MC2 was due to apoptosis, typical markers of apoptosis were analyzed in response to VCR and/or MC2. Then we analyzed nuclei fragmentation by DAPI staining and investigated the expression level of Bcl-2, Bax and PARP by western-blot. As shown in Figure 4A, at a concentration of 16 μM of MC2 and 0.2 μM VCR, neither drug caused significant morphological changes of apoptosis in KB/VCR cells. In contrast, treatment of KB/VCR cells with the combination of MC2 and VCR resulted in increase in the fraction of apoptotic cells with condensed and fragmented DNA (as indicated by a stronger blue fluorescence). Given the profound roles of the Bcl-2 family in triggering apoptosis,[22] we next examined if antiapoptotic protein Bcl-2, and proapoptotic protein Bax were involved in combination treatment-induced apoptosis. The results in Figure 4B indicated that neither MC2 nor VCR alone had any detectable effect on the expression of Bcl-2 and Bax, however, the combination treatment of MC2 with VCR led to noticeable down-regulation of Bcl-2 and up-regulation of Bax in KB/VCR cells. In addition, alterations in expression of Bcl-2 family members may trigger the activation of caspases, which, in turn, lead to cleavage of poly (ADP-ribose) polymerase (PARP), another hallmark of the apoptotic response.[23] Accordingly, the results in Figure 4B indicated that the native 116 kDa PARP protein was cleaved into its characteristic 85 kDa fragment upon treatment with MC2 and VCR. These results suggested that the enhanced inhibitory effect on KB/VCR cells by the combination of MC2 and VCR was achieved through a concomitant increase in apoptosis.

3. Discussions

In the past two decades, a number of natural and synthetic compounds have been tested for their ability to reverse MDR. Although several chemosensitizers have been shown to be very potent in reversal of MDR in both in vitro and in vivo experiments, the results of clinical trials with these compounds were disappointing because of the side effects and/or weak potency.[4,24,25] The aim of this study was to continue our work to identify novel naturally-occurring chemicals that exert anti-tumor activity and/or reverse multidrug resistance.

In the present study, we showed for the first time that MC and its synthetic derivatives significantly increased the sensitivity of KB/VCR cells toward VCR. Especially MC2, showed the largest potency to enhance VCR cytotoxicity in drug resistance cells with the reversal fold of 4.7–7.5. In order to understand the underlined mechanism of reversal of MDR of this class of compounds, the most active compound MC2 was employed as the tested drug. The results showed that MC2 enhanced the cytotoxicity of VCR and ADR toward KB/VCR cells, whereas MC2 in concentrations ranging from 5 to 50 μM did not display any significant anti-proliferative effect on both drug-sensitive KB and drug-resistant KB/VCR cells. Thus, the low cytotoxicity provides the foundation property for MC2 because MDR modulators would better not have cytotoxic or off-target effects.

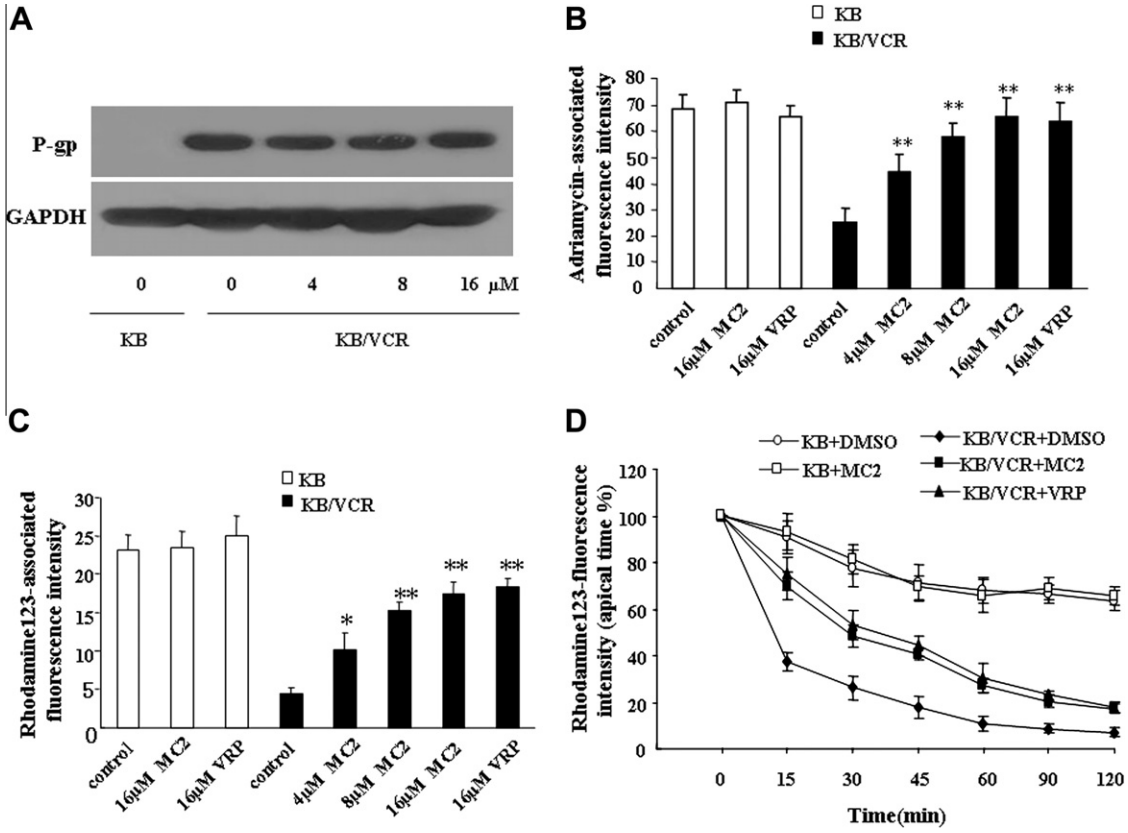

Figure 3. (A) Effect of MC2 on the expression of *P*-gp. KB/VCR cells were treated with MC2 at 4, 8, 16 μM for 48 h. Total cell proteins (50 μg) were separated by SDS–PAGE, and then transferred to PVDF membrane. The membranes were immunoblotted with *P*-gp antibody. Immunoreactive proteins were visualized using an ECL. (B) Effect of MC2 on ADR accumulation in KB and KB/VCR cells. Cells were treated with 3 μg/ml ADR in the absence and presence of MC2 for 1 h. Intracellular accumulation of ADR was evaluated by measuring the mean fluorescence intensity. (C) MC2 increased the accumulation of Rh123 in KB/VCR cells. Cells were pretreated with 4, 8, 16 μM of MC2 for 1 h and then were exposed to 2 mg/mL of Rh123 for another 1 h. Rh123-associated fluorescence intensity was determined by flow cytometry. Data were expressed as means ± S.D. of three independent experiments. $^{*}P<0.05$ and $^{**}P<0.01$ versus DMSO treated KB/VCR cells. (D) MC2 blocked intracellular Rh123 efflux in KB/VCR cells. Cells were exposed to 5 μM of Rh123 in the presence of MC2 or VRP at 37 °C for 60 min. The cells were then washed three times with medium without Rh123, Cells were collected at 15, 30, 45, 60, 90, 120 min, respectively, and resuspended in 1 mL of ice-cold PBS. Rh123-associated fluorescence intensity was analyzed by flow cytometry.

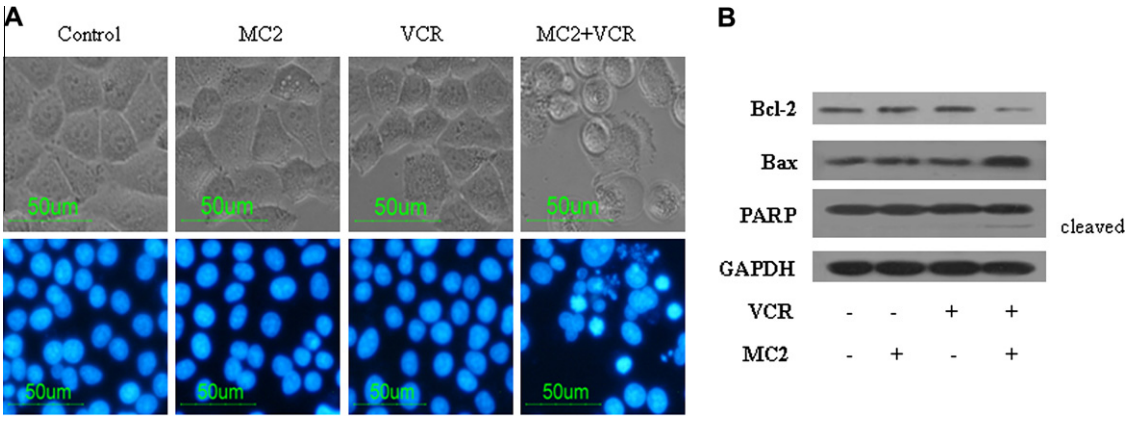

Figure 4. (A) MC2 treatment increased VCR-induced apoptosis in drug-resistant KB/VCR cells. Cells were treated with 16 μM MC2, 0.2 μM VCR, or the combination of 16 μM MC2 and 0.2 μM VCR for 48 h. After fixation, cells were stained with DAPI and cell morphological characterization was analyzed using fluorescence microscope. (B) The expression levels of Bax, Bcl-2 and PARP in KB/VCR cells after treatment with 16 μM MC2, 0.2 μM VCR, or the combination of 16 μM MC2 and 0.2 μM VCR for 48 h. Total cell proteins (50 μg) were separated by SDS–PAGE, and then transferred to PVDF membrane. The membranes were immunoblotted with desired antibody. Immunoreactive proteins were visualized using an ECL.

The results above indicated that MC2 could enhance the sensitivity of *P*-gp-overexpressing cells to certain chemotherapeutic agents. The mechanism by which this occurs is unknown. The reversal of *P*-gp-mediated MDR can be achieved either by decreasing *P*-gp expression or by inhibiting its activity.[26] We firstly studied the effect of MC2 on *P*-gp expression. The result of Western blot showed that the protein level of *P*-gp in KB/VCR cells was not altered by MC2 treatment. This experiment suggested that MC2 didn't affect the expression of *P*-gp in KB/VCR cells. So we then examined its effect on the drug-transport function of *P*-gp.

As shown in Figure 3, the transport of ADR and Rh123 by *P*-gp is significantly inhibited by MC2 in a concentration-dependent manner. The treatment of MC2 resulted in a remarkable increment of the fluorescent intensity from ADR and Rh123 in KB/VCR cells, indicating that MC2 elevated accumulation of ADR and Rh123 in KB/VCR cells. However, the accumulation level of ADR and Rh123 was hardly varied in KB cells no matter with or without MC2 treatment. These supported the notion that the enhanced cytotoxicity of chemotherapeutic agents by MC2 was attributed to its inhibition activity to *P*-gp.

The above results showed that MC2 could inhibit the function of *P*-gp. The question if MC2 may act as direct inhibitor of *P*-gp function or as *P*-gp substrate was addressed by Rh123 efflux assay. The time kinetics of MC2-mediated inhibition of Rh123 efflux was investigated in KB/VCR cells. Whereas *P*-gp inhibitors commonly show prolonged activity even after a washing out period, the activity of *P*-gp substrates rapidly declines after substance removal.[27,28] To examine this, cells were incubated with Rh123 in the presence of MC2 or VRP for 60 min. Then, cells were washed and Rh123 fluorescence was detected after 0, 15, 30, 45, 60, and 120 min. Results indicated that Rh123 fluorescence decreases after wash-out of MC2 or VRP. Noteworthy, MC2-induced effects on Rh123 accumulation were similar to those induced by VRP that is known to inhibit *P*-gp being a *P*-gp substrate. Taken together, these results suggest that MC2 acts as a *P*-gp transport substrate.

An important aspect of cancer chemotherapy is based on the abilities of chemotherapeutic agents to induce apoptosis in cancer cells.[29,30] In addition to evaluate the effect of MC2 on *P*-gp transport function, we examined the effect of MC2 on VCR cytotoxicity. The combination treatment of MC2 with VCR markedly induced apoptosis. However, treatment of the cells with MC2 (16 μM) or VCR (0.2 μM) alone did not trigger apoptosis under the same condition. The result suggested that the increased inhibitory effect on KB/VCR cells from the combination of MC2 with VCR was achieved through the action of MC2, which enhanced the VCR-induced apoptosis. To further investigate the possible mechanism of action by which MC2 potentiated cytotoxicity of VCR, we evaluated the expression level of Bcl-2 and Bax through Western blot analysis. The results showed that the expression of proapoptotic protein Bax was significantly up-regulated and antiapoptotic protein Bcl-2 was decreased by the combination treatment of VCR with MC2. This result suggested that combination treatment-induced apoptosis in KB/VCR cells is partly mediated by the Bcl-2 family. Additionally, typical processing of PARP into the 85-kDa fragment was also observed when KB/VCR cells were treated with VCR in the presence of MC2. These phenomena confirmed the results of the MTT assay. Future research is required to analyze the action of MC2 in other MDR cell lines as well as in animal models.

In conclusion, the present study shows that marchantin C and its synthetic derivatives significantly reverse *P*-gp-mediated MDR in cancer cells. Of four derivatives, MC2 exhibited more potent effects on MDR reversal by inhibiting the drug efflux function of *P*-gp, resulting in the increase of the intracellular accumulation of the anticancer drugs. The low cytotoxicity, non-interference on the expression of *P*-gp, and reversible blocking action of *P*-gp suggest that MC2 is a promising candidate for further investigation.

4. Experimental

4.1. General procedures

Column chromatography was carried out on silica gel or alumina (200–300 mesh). Reactions were monitored by thin-layer chromatography, using Merck plates with a fluorescent indicator. Melting points were determined on an X-6 melting-point apparatus and are uncorrected. The ^{1}H NMR spectra were recorded on a Bruker Spectospin spectrometer at 300 or 600 MHz, using TMS as an internal standard. The chemical shifts are reported in parts per million (ppm δ) referenced to the residual ^{1}H resonance of the solvent ($CDCl_3$, 7.26 ppm). Abbreviations used in the splitting pattern were as follows: s = singlet, d = doublet, t = triplet, quin = quintet, m = multiplet, and br = broad. Reagents were used as purchased without further purification. Solvents (THF, CH_2Cl_2 and CH_3CN) were dried and freshly distilled before use according to procedures reported in the literature.

4.2. Synthesis

4.2.1. 2-(1,3-Dioxan-2-yl)-6-methoxyphenol (2)

2-Hydroxy-3-methoxybenzaldehyde (**1**, 9.12 g, 0.06 mol) was added to a well-stirred solution of DMS–DMF adduct (15.99 g, 0.08 mol) and 1,3-propanediol (14.05 g, 0.18 mol) in CH_2Cl_2 (40 mL), the resulting mixture was then stirred for 24 h at room temperature, and slowly quenched with Et_3N (11 mL, 0.08 mol) at 0 °C. The reaction mixture was extracted with Et_2O (50 mL × 5) and the combined organic layer was washed with NaOAc–saturated 5% aqueous $NaHSO_3$ (25 mL × 3) and NaOAc-saturated brine (25 mL × 2), and then dried over anhydrous sodium sulfate. The solvent was evaporated to yield a white solid (10.83 g, 86%) that was recrystallized from CH_2Cl_2 and hexane: mp white solid; mp 105–106 °C. ^{1}H NMR (300 MHz, $CDCl_3$) δ 7.00 (dd, J = 4.2 Hz, 5.4 Hz, 1H), 6.86 (s, 1H), 6.84 (d, J = 1.8 Hz, 1H), 5.78 (s, 1H), 4.29 (dd, J = 4.8 Hz, 12.0 Hz, 2H), 4.03 (dt, J = 2.4 Hz, 12.6 Hz, 2H), 3.87 (s, 3H), 2.33–2.20 (m, 1H), 1.49–1.46 (m, 1H); MS (ESI) 211 $(M+H)^+$.

4.2.2. 3-(2-(1,3-Dioxan-2-yl)-6-methoxyphenoxy)benzaldehyde (3)

A mixture of 2-(1,3-dioxan-2-yl)-6-methoxy-phenol (**2**, 10 g, 0.05 mol), 3-bromo-benzaldehyde (8.8 g, 0.05 mmol), potassium carbonate (13.5 g, 0.09 mol) and cupric oxide (0.95 g, 5.9 mmol) in pyridine (50 mL) was stirred under reflux for 12 h. The pyridine was distilled off in vacuo and the residue was extracted with ethyl acetate (200 mL). The solution was concentrated and the residue was purified by flash column chromatography (Al_2O_3), eluting with a 2:1 solution of petroleum ether–CH_2Cl_2 to afford **3** (12.6 g, 81%) as a yellow solid; white solid; mp 105–106 °C. ^{1}H NMR (300 MHz, $CDCl_3$) δ 9.95 (s, 1H), 7.55 (d, J = 7.2 Hz, 1H), 7.43 (t, J = 7.8 Hz, 1H), 7.37 (d, J = 8.4 Hz, 2H), 7.30 (t, J = 7.8 Hz, 1H), 7.15 (d, J = 5.4 Hz, 1H), 7.02 (d, J = 7.8 Hz, 1H), 5.69 (s, 1H), 4.14 (d, J = 7.8 Hz, 2H), 3.85 (t, J = 12.0 Hz, 2H), 3.74 (s, 3H), 2.21–2.16 (m, 1H), 1.37 (d, J = 13.2 Hz, 1H); MS (ESI) 315 $(M+H)^+$.

4.2.3. Methyl 4-(5-formyl-2-methoxyphenoxy) benzoate (6)

This compound was prepared from methyl 4-bromobenzoate (15.05 g, 69.98 mmol) and 3-hydroxy-4-methoxybenzaldehyde (10.63 g, 69.98 mmol) by means of a procedure similar to that used for **3**. After concentration of the solution, the residue was purified by flash column chromatography (SiO_2), eluting with a 3:2 solution of petroleum ether–CH_2Cl_2 to afford **6** (15.86 g, 79%) as an orange solid; mp 118–120 °C. ^{1}H NMR (300 MHz, $CDCl_3$) δ 9.87 (s, 1H), 8.02–7.99 (m, 2H), 7.76 (dd, J = 8.2, 2.1 Hz, 1H), 7.59 (d, J = 2.1 Hz, 1H), 7.14 (d, J = 8.3 Hz, 1H), 6.94 (d, J = 8.7 Hz, 2H), 3.91 (s, 3H), 3.90 (s, 3H); MS (ESI) 287 $(M+H)^+$.

4.2.4. Methyl 4-(5-(hydroxymethyl)-2-methoxyphenoxy) benzoate (7)

Sodium borohydride (0.68 g, 18.32 mmol) was added to a solution of **6** (12.87 g, 45.73 mmol) in THF (40 mL) over 15 min at 0 °C. The reaction mixture was then stirred at room temperature for 3 h. Water (10 mL) and 1 M HCl (18 mL) were added and the THF was evaporated in vacuo. The resulting mixture was extracted with

CH_2Cl_2 (20 mL), washed with satd aq NaCl (10 mL × 3), and dried over sodium sulfate. The solution was concentrated to obtain a crude oil that was purified by flash column chromatography (SiO_2), eluting with CH_2Cl_2 to afford **7** (11.87 g, 91%) as a white solid; mp 77–79 °C. ^{1}H NMR (300 MHz, $CDCl_3$) δ 7.97 (d, J = 8.7 Hz, 2H), 7.21 (dd, J = 8.1, 1.8 Hz, 1H), 7.09 (d, J = 1.8 Hz, 1H), 7.00 (d, J = 8.1 Hz, 1H), 6.92 (d, J = 8.7 Hz, 2H), 4.63 (s, 2H), 3.89 (s, 3H), 3.80 (s, 3H), 1.67 (br s, 1H); MS (ESI) 289 $(M+H)^+$.

4.2.5. (4-Methoxy-3-(4-(methoxycarbonyl)phenoxy)benzyl)triphenylphosphonium bromide (8)

Methyl 4-(5-(hydroxymethyl)-2-methoxyphenoxy) benzoate (**7**, 7.06 g, 24.5 mmol) and triphenylphosphonium bromide (8.40 g, 24.5 mmol) was dissolved in anhydrous CH_3CN (50 mL), the resulting mixture was then refluxed for 3 h, the solvent was removed in vacuo and the residue was purified by silica gel column chromatography, eluting with 5% ethanol in dichloromethane, to yield **8** (13.21 g, 88%) as a white solid; mp 217–219 °C. ^{1}H NMR (300 MHz, $CDCl_3$) δ 7.90 (d, J = 9.0 Hz, 2H), 7.80–7.73 (m, 9H), 7.65–7.58 (m, 6H), 7.27 (s, 1H), 6.84 (d, J = 8.4 Hz, 1H), 6.69 (d, J = 8.7 Hz, 2H), 6.51 (s, 1H), 5.46 (d, J = 14 Hz, 2H), 3.90 (s, 3H), 3.73 (s, 3H); MS (ESI) 533 $(M-Br)^+$.

4.2.6. Methyl4-(5-(3-(2-(1,3-dioxan-2-yl)-6-methoxyphenoxy)phenethyl)-2-methoxyphenoxy)benzoate (10)

Potassium carbonate (8.89 g, 64.44 mmol) and a trace of 18-crown-6 were added to a solution of **3** (10.12 g, 32.22 mmol) and **8** (19.72 g, 32.22 mmol) in anhydrous CH_2Cl_2 (80 mL), the resulting mixture was stirred under reflux for 24 h. The insoluble material was then filtered off and the filtrate was concentrated to provide the orange oil that was purified by flash column chromatography (Al_2O_3), eluting with a 3:1 solution of hexane–CH_2Cl_2 to afford **9** (16.87 g, 92%) as a yellow oil. Pd/C 10% (1.5 g) and triethylamine (35 mL) were then added to a solution of **9** (15 g, 26.41 mmol) in ethyl acetate (200 mL). The suspension was stirred under H_2 for 24 h at room temperature. The mixture was filtered, and concentration provided a crude yellow solid that was purified by precipitating from ethyl ether-petroleum ether to afford **10** (14.7 g, 97%) as a white solid; mp 89–90 °C. ^{1}H NMR (600 MHz, $CDCl_3$) δ 7.99 (d, J = 8.4 Hz, 2H), 7.36 (d, J = 7.8 Hz, 1H), 7.27 (d, J = 8.4 Hz, 1H), 7.15 (t, J = 7.8 Hz, 1H), 7.02 (d, J = 8.4 Hz, 1H), 7.01 (d, J = 8.4 Hz, 1H), 6.94 (d, J = 8.4 Hz, 1H), 6.89 (d, J = 8.4 Hz, 2H), 6.86 (d, J = 1.8 Hz, 1H), 6.77 (d, J = 7.8 Hz, 1H), 6.70 (dd, J = 2.4 Hz, 8.4 Hz, 1H), 5.68 (s, 1H), 4.17–4.14 (m, 2H), 3.91 (s, 3H), 3.83 (s, 2H), 3.78 (s, 3H), 3.71 (s, 3H), 2.85 (s, 4H), 2.24–2.16 (m, 1H), 1.35 (d, J = 13.2 Hz, 1H); MS (ESI) 571 $(M+H)^+$.

4.2.7. (4-(5-(3-(2-Formyl-6-methoxyphenoxy)phenethyl)-2-methoxyphenoxy)benzyl)triphenylphosphonium bromide (12)

A solution of **10** (13.35 g, 23.86 mmol) in anhydrous THF (25 mL) was added dropwise to a stirred suspension of lithium aluminum hydride (1.79 g, 46.98 mmol) in anhydrous THF (30 mL). The resulting mixture was stirred at room temperature for 2.5 h and carefully hydrolysed with satd aq ammonium chloride (10 mL). THF was removed in vacuo and the resulting mixture was diluted with CH_2Cl_2 (100 mL), washed with satd aq NaCl (20 mL × 3) and dried over sodium sulfate. The solution was concentrated to obtain a crude oil that was subsequently dissolved in a solution of ethanol (100 mL) and 10% aq HCl (20 mL). The resulting mixture was then stirred at room temperature for 12 h. Satd aq sodium bicarbonate (150 mL) was added and the ethanol was removed in vacuo. The resulting mixture was extracted with CH_2Cl_2 (200 mL), washed with satd aq NaCl (25 mL × 3) and dried over sodium sulfate. The solution was concentrated to yield **11** (9.74 g, 87%) as colorless oil. Compound **11** (10 g, 20.7 mmol) then reacted with triphenylphosphonium bromide (7.08 g, 20.7 mmol) by means of a procedure similar to that used for **8** to yield **12** (13.93 g, 83%) as a white solid; mp 229–230 °C. ^{1}H NMR (600 MHz, $CDCl_3$) δ 10.22 (s, 1H), 7.77–7.65 (m, 15H), 7.53 (d, J = 6.6 Hz, 1H), 7.33–7.29 (m, 3H), 7.14 (t, J = 7.8 Hz, 1H), 7.04 (d, J = 7.8 Hz, 2H), 6.86 (s, 2H), 6.81 (d, J = 7.2 Hz, 1H), 6.71 (s, 1H), 6.68 (d, J = 7.8 Hz, 2H), 6.63 (s, 1H), 5.40 (d, J = 13.8 Hz, 2H), 3.80 (s, 3H), 3.77 (s, 3H), 2.80 (s, 4H); MS (ESI) 533 $(M-Br)^+$.

4.2.8. Dimethyl ether of dehydromarchantin C (13)

A solution of **12** (1.13 g, 1.41 mmol) in anhydrous CH_2Cl_2 (150 mL) was added dropwise to a stirred suspension of sodium methoxide (152 mg, 2.82 mmol) in anhydrous CH_2Cl_2 (200 mL) over 7 h and the reaction mixture was stirred for 5 h at room temperature. The reaction mixture was filtered, concentrated and the residue was purified by silica gel column chromatography, eluting with CH_2Cl_2 to yield **13** (0.54 g, 86%) as a white solid; mp 225–226 °C. ^{1}H NMR (600 MHz, $CDCl_3$) δ 7.23–7.15 (m, 3H), 7.09 (d, J = 7.5 Hz, 1H), 6.98–6.6.89 (m, 4H), 6.84 (d, J = 7.8 Hz, 2H), 6.77 (d, J = 8.4 Hz, 1H), 6.65 (d, J = 15.9 Hz, 1H), 6.53 (d, J = 9.0 Hz, 1H), 6.47 (d, J = 15.9 Hz, 1H), 6.10 (d, J = 8.7 Hz, 1H), 5.66 (s, 1H), 3.95 (s, 1H), 3.89 (s, 1H), 2.97–2.87 (m, 4H); MS (ESI) 451 $(M+H)^+$.

4.2.9. Dimethyl ether of marchantin C (14)

Pd/C 10% (250 mg) were added to a solution of **13** (2.25 g, 5.34 mmol) in ethyl acetate (150 mL). The suspension was stirred under H_2 for 24 h at room temperature. The reaction mixture was filtered, and the solution was concentrated to provide the crude product that was recrystallized from ethanol to yield **14** (2.2 g, 95%) as a white solid; mp 150–151 °C. ^{1}H NMR (600 MHz, $CDCl_3$) δ 7.23 (t, J = 7.8 Hz, 1H), 7.11 (d, J = 7.8 Hz, 1H), 6.95 (d, J = 7.8 Hz, 2H), 6.92 (t, J = 7.8 Hz, 1H), 6.86 (t, J = 8.4 Hz, 2H), 6.80 (d, J = 8.4 Hz, 1H), 6.64 (d, J = 7.2 Hz, 2H), 6.62 (s, 1H), 6.45 (d, J = 8.4 Hz, 1H), 6.26 (d, J = 7.2 Hz, 1H), 5.49 (s, 1H), 3.93 (s, 3H), 3.70 (s, 3H), 3.06 (s, 3H), 2.85–2.79 (m, 4H); MS (ESI) 453 $(M+H)^+$.

4.2.10. Dehydromarchantin C (15)

A solution of boron tribromide (1.95 g, 7.83 mmol) in anhydrous CH_2Cl_2 (10 mL) was added dropwise to a stirred solution of **13** (0.44 g, 0.98 mmol) in anhydrous CH_2Cl_2 (10 mL) at −78 °C. The reaction mixture was stirred at −78 °C for 3 h, and then was allowed to warm up to room temperature within 12 h. The ice-cold water was added, and the reaction mixture was stirred vigorously for 1 h. The solution was then diluted with CH_2Cl_2 (50 mL), washed with satd aq NaCl (20 mL × 3) and dried over sodium sulfate. The solution was concentrated, and the residue was purified by flash column chromatography (SiO_2), eluting with CH_2Cl_2 to yield **15** (0.31 g, 73%) as a white solid; mp 101–102 °C. ^{1}H NMR (600 MHz, $CDCl_3$) δ 7.18 (d, J = 9.0 Hz, 2H), 7.12 (t, J = 9.0 Hz, 1H), 7.04 (t, J = 9.6 Hz, 2H), 6.93 (d, J = 3.0 Hz, 2H), 6.91 (d, J = 3.0 Hz, 2H), 6.89 (d, J = 7.8 Hz, 1H), 6.77 (d, J = 7.8 Hz, 1H), 6.70 (d, J = 16.2 Hz, 1H), 6.57 (d, J = 7.8 Hz, 1H), 6.36 (d, J = 16.2 Hz, 1H), 6.19 (dd, J = 1.8 Hz, 8.4 Hz, 1H), 5.65 (s, 1H), 6.53 (d, J = 9.0 Hz, 1H), 6.47 (d, J = 15.9 Hz, 1H), 6.10 (d, J = 8.7 Hz, 1H), 5.66 (s, 1H), 3.95 (s, 1H), 3.89 (s, 1H), 3.02–2.93 (m, 4H); ^{13}C NMR (600 MHz, $CDCl_3$) δ 157.9, 154.6, 148.9, 148.0, 143.2, 143.1, 139.3, 137.9, 134.1, 131.8, 131.6, 131.1, 128.8, 127.0, 125.8, 122.8, 122.6, 120.3, 117.4, 117.0, 115.1, 114.8, 113.8, 112.9, 33.8, 30.5; MS (ESI) 423 $(M+H)^+$.

4.2.11. Marchantin C (16)

This compound was prepared from compound **13** (0.60 g, 1.33 mmol) by means of a procedure similar to that used for **15**. Compound **16** (0.37 g, 89%) was obtained as a white solid; mp 148–149 °C. ^{1}H NMR (600 MHz, $CDCl_3$) δ 7.11 (t, J = 7.8 Hz, 1H),

7.05 (dd, J = 7.8 Hz, 1.8 Hz, 1H), 6.98 (d, J = 8.5 Hz, 2H), 6.97 (t, J = 7.8 Hz, 1H), 6.85 (dd, J = 7.8 Hz, 1.8 Hz, 1H), 6.83 (d, J = 8.1 Hz, 1H), 6.58 (t, J = 2.1 Hz, 1H), 6.56 (d, J = 8.5 Hz, 2H), 6.55 (dt, J = 7.8 Hz, 2.1 Hz, 1H), 6.35 (d, J = 7.8 Hz, 1H), 5.64 (d, J = 2.0 Hz, 1H), 3.01–3.05 (m, 4H), 2.85 (m, 2H), 2.75 (m, 2H); ^{13}C NMR (600 MHz, $CDCl_3$) δ 156.7, 152.8, 148.6, 146.1, 143.4, 143.0, 139.6, 139.1, 136.1, 132.6, 129.7, 128.9, 126.1, 123.4, 122.4, 122.0, 121.3, 115.6, 115.4, 114.9, 114.3, 112.0, 35.8, 35.3, 34.0, 30.3; MS (ESI) 425 $(M+H)^+$.

4.3. Chemical preparation

MC (**16**) and its derivatives (**13**, **14**, and **15**, namely MC1, MC2 and MC3) were dissolved in dimethylsulfoxide (DMSO, Sigma-Aldrich) and stored as small aliquots at −20 °C. Rhodamine123 (Rh123), 3-(4,5-dimethylthiazol)-2,5-diphenyltetrazolium bromide (MTT), and verapamil (VRP) were purchased from Sigma Co, USA. Adriamycin (ADR) and vincristine (VCR) were purchased from Zhejiang Haizheng Pharmaceutical Factory (Zhejiang, China), and prepared in sterile deionized H_2O. The stock solutions were stored as aliquots at −20 °C.

4.4. Cell culture

Human epidermoid carcinoma KB cells and its VCR resistant KB/VCR cells[31] with characteristics of MDR attributable to expression of *P*-gp (a gift from Dr. J. Ding, Shanghai Institute of Materia Medica, Chinese Academy of Sciences, Shanghai, China) were routinely cultured in RPMI-1640 medium supplemented with 10% fetal bovine serum, 100 U/mL penicillin-G, and 100 μg/mL streptomycin at 37 °C in a humidified atmosphere containing 5% CO_2. KB/VCR cells were, maintained in medium containing 200 ng/mL VCR and incubated in drug-free medium for at least one week prior to experiments.

4.5. Cytotoxicity and multidrug resistance reversal assay

Cells were seeded into 96-well plates and exposed to varying concentrations of MC, MC1, MC2 and MC3, respectively. The cytotoxicity was analyzed after treatment of cells with these compounds for 48 h by MTT assay. Control cells were subjected to DMSO treatment. In MDR reversing assay, cells seeded in 96-well plates were treated with VCR alone, or VCR combined with various concentrations of target compounds for 48 h, cell proliferation was assessed using MTT assay. Verapamil (VRP) was included as a reference agent. The IC_{50} values were defined as the drug concentration that resulted in a 50% inhibition of cell growth using untreated cells as 100%. Reversal fold index (RF) was calculated as the ratio, RF = IC_{50} of VCR alone/IC_{50} of VCR combined with desired chemicals.

4.6. Intracellular adriamycin accumulation

Accumulation of adriamycin (ADR) was determined by incubating tumor cells with ADR (3 μg/mL) alone or in combination with MC2 (4, 8, 16 μM, respectively) for 1 h at 37 °C. Cells were then placed in ice-water bath to stop the reaction followed by harvesting and washing twice with ice-cold PBS. The intracellular ADR concentration was determined by monitoring a change in fluorescence intensity associated with ADR using FACScan flow cytometry. Data analysis was completed with Cell Quest software.

4.7. Rh123 accumulation and efflux assay

Effect of MC2 on the intracellular accumulation of Rh123 was determined as previously described. KB and KB/VCR cells were treated with MC2 (4, 8, 16 μM) or DMSO for 1 h before the addition of Rh123 (5 μM) at 37 °C, and the cells were maintained for an additional 1 h in the dark. After washing with cold PBS, the cells were then resuspended in 1 ml of ice-cold PBS for analysis using flow cytometry. Fluorescence intensity associated with Rh123 was measured using FACScan caliber equipped with a 488 nm argon laser. The emitted fluorescence was measured by a 530 nm band-pass filter.

In the efflux study, KB and KB/VCR cells were cultured with medium containing 5 μM of Rh123 in the presence of MC2 or VRP at 37 °C for 60 min, respectively. The cells were then washed three times with normal growth medium without Rh123. Cells were collected at 15, 30, 45, 60, 90, 120 min, respectively, and resuspended in 1 mL of ice-cold PBS. Rh123-associated fluorescence intensity was analyzed by flow cytometry.

4.8. Western blot analysis

After treatment with MC2 or VCR as indicated for 24 h, cells were washed with ice-cold PBS and cell lysates were prepared using RIPA buffer containing fresh protease inhibitor mixture (50 μg/mL aprotinin, 0.5 mM phenylmethanesulfonyl fluoride (PMSF), 1 mM sodium orthovanadate, 10 mM sodium fluoride and 10 mM β-glycerolphosphate). Proteins were quantified using the BCA protein assay. Samples containing equal amounts of protein (100 μg) from lysates were separated by SDS–PAGE and electrophoretically transferred onto polyvinylidene fluoride (PVDF) membranes. After being blocked with 5% fat-free dry milk in TBST (20 mM Tris–HCl (pH 7.6), 150 mM NaCl and 0.1% Tween 20) for 1 h at room temperature, the membranes were immunoblotted overnight with specific antibodies against *P*-gp, Bcl-2, Bax, or poly (ADP-ribose) polymerase (PARP) (Santa Cruz Biotech, USA), respectively, followed by incubation with HRP-conjugated secondary antibodies for 1 h at room temperature. Membranes were stripped and reprobed with Glyceraldehyde-3-phosphate dehydrogenase (GAPDH) (Santa Cruz Biotechnology) as a protein loading control. Membranes were visualized by enhanced chemiluminescence detection system (Millipore) and followed by exposure to X-ray films.

4.9. DAPI staining

Nucleic morphological changes of apoptosis were determined by staining cell with DAPI. Cells were seeded into 24-well plates and treated with MC2 (16 μM), VCR (0.2 μM) or a combination of MC2 (16 μM) with VCR (0.2 μM) for 48 h. After washing with PBS, cells were fixed with 4% paraformaldehyde (Sigma) in PBS for 10 min at room temperature. The fixed cells were then washed with PBS and permeabilized with 0.1% Triton X-100 for 10 min prior to staining with DAPI (1:2000 dilution, in 1 × PBS) for 10 min. The cells were washed with PBS and mounted. Images of DAPI fluorescence were collected using a Nikon phase-fluorescence microscope.

4.10. Statistical analysis

Data were expressed as means ± SD. Statistical analysis of the data was performed using the Student's t test. p <0.05 was considered statistically significant.

Acknowledgments

This work was supported by the National Natural Science Foundation of China (30973551), Shandong Provincial Key Research Foundation (2006GG1102023 and 2008GG10002042), and Foundation for the Young Researcher Program of the Health Department of Shandong Province (2006J39).

References and notes

1. Borowski, E.; Bontemps-Gracz, M. M.; Piwkowska, A. *Acta Biochim. Pol.* **2005**, *52*, 627.
2. O'Connor, R. *Anticancer Res.* **2007**, *27*, 1267.
3. Donnenberg, V. S.; Donnenberg, A. D. *J. Clin. Pharmacol.* **2005**, *45*, 872.
4. Gottesman, M. M. *Annu. Rev. Med.* **2002**, *53*, 615.
5. Szakacs, G.; Paterson, J. K.; Ludwig, J. A. *Nat. Rev. Drug Disc.* **2006**, *5*, 219.
6. Teodori, E.; Dei, S.; Martelli, C.; Scapecchi, S.; Gualtieri, F. *Curr. Drug Targets* **2006**, *7*, 893.
7. Di Pietro, A.; Conseil, G.; Pérez-Victoria, J. M.; Dayan, G.; Baubichon-Cortay, H.; Trompier, D. *Cell Mol. Life Sci.* **2002**, *59*, 307.
8. Chearwaw, W.; Anuchapreeda, S.; Nandigama, K.; Ambudkar, S. V.; Limtrakul, P. *Biochem. Pharmacol.* **2004**, *68*, 2043.
9. Kitagawa, S. *Biol. Pharm. Bull.* **2006**, *29*, 1.
10. Asakawa, Y. *Phytochemistry* **2001**, *56*, 297.
11. Baek, S. H.; Phipps, R. K.; Perry, N. B. *J. Nat. Prod.* **2004**, *67*, 718.
12. Burgess, E. J.; Larsen, L.; Perry, N. B. *J. Nat. Prod.* **2000**, *63*, 537.
13. Asakawa, Y.; Toyota, M.; Matsuda, R.; Takikawa, K.; Takemoto, T. *Phytochemistry* **1983**, *22*, 1413.
14. Asakawa, Y.. In *Progress in the Chemistry of Organic Natural Products*; Springer, 1995; Vol. 65.
15. Asakawa, Y.; Toyota, M.; Tori, M.; Hashimoto, T. *Spectroscopy* **2000**, *14*, 149.
16. Scher, J. M.; Burgess, E. J.; Lorimer, S. D.; Perry, N. B. *Tetrahedron* **2002**, *58*, 7875.
17. Harinantenaina, L.; Quang, D. N.; Takeshi, N.; Hashimoto, T.; Kohchi, C.; Soma, G. I.; Asakawa, Y. *J. Nat. Prod.* **2005**, *68*, 1779.
18. Harinantenaina, L.; Kida, S.; Asakawa, Y. *Arkivoc* **2007**, *vii*, 22.
19. Shi, Y. Q.; Liao, Y. X.; Qu, X. J.; Yuan, H. Q.; Li, S.; Qu, J. B.; Lou, H. X. *Cancer Lett.* **2008**, *262*, 173.
20. Shi, Y. Q.; Zhu, C. J.; Yuan, H. Q.; Li, B. Q.; Gao, J.; Qu, X. J.; Sun, B.; Cheng, Y. N.; Li, S.; Li, X.; Lou, H. X. *Cancer Lett.* **2009**, *276*, 160.
21. Speicher, A.; Holz, J. *Tetrahedron Lett.* **2010**, *51*, 2986.
22. Richardson, A.; Kaye, S. B. *Curr. Mol. Pharmacol.* **2008**, *1*, 244.
23. Rouleau, M.; Patel, A.; Hendzel, M. J.; Kaufmann, S. H.; Poirier, G. G. *Nat. Rev. Cancer* **2010**, *10*, 293.
24. Takara, K.; Sakaeda, T.; Okumura, K. *Curr. Pharm. Des.* **2006**, *12*, 273.
25. Volm, M. *Anticancer Res.* **1998**, *18*, 2905.
26. Shi, Z.; Peng, X. X.; Kim, I. W. *Cancer Res.* **2007**, *67*, 11012.
27. Ludwig, J. A.; Szaka′cs, G.; Martin, S. E. *Cancer Res.* **2006**, *66*, 4808.
28. Newman, M. J.; Rodarte, J. C.; Benbatoul, K. D. *Cancer Res.* **2000**, *60*, 2964.
29. Bhandari, M. S.; Petrylak, D. P.; Hussain, M. *Eur. J. Cancer* **2005**, *41*, 941.
30. Ciechomska, I.; Pyrzynska, B.; Kazmierczak, P.; Kaminska, B. *Oncogene* **2003**, *22*, 7617.
31. Miao, Z. H.; Tang, T.; Zhang, Y. X.; Zhang, J. S.; Ding, J. *Int. J. Cancer* **2003**, *106*, 108.